On the frequency dependence of UWB indoor channel parameters : 3D ray tracing and measurement

Edgard Haddad, Nadine Malhouroux-Gaffet, Patrice Pajusco, Michel Ney

On the Frequency Dependence of UWB Indoor Channel Parameters: 3D Ray Tracing and Measurement

Edgar Haddad[*], Nadine Malhouroux[*], Patrice Pajusco[+], Michel Ney[+]

[*]*Wireless Engineering and Propagation department, Orange Labs*
6 av. des usines, 90007 Belfort Cedex, France
{edgar.haddad, nadine.malhouroux}@orange-ftgroup.com

[+]*Telecom Bretagne, Lab STICC*
CS 83818, 29238 Brest Cedex, France
{patrice.pajusco, michel.ney}@telecom-bretagne.eu

***Abstract*— In this paper, measurements and 3D ray tracing predictions of multiple input multiple output (MIMO) ultra wideband (UWB) channel parameters in a residential area are presented. The studied UWB channel parameters, i.e. the delay spread and the azimuth and elevation angular spreads, are absolutely required in propagation modeling during the specification phase of future mobile MIMO communications systems. The evolution of the predicted parameters with the number and type of interactions of the simulated channel is also presented. Then, we focus on the frequency dependence of the predicted parameters and compare it with the measurement. Results show limited variations with increasing frequency. This implies that most of indoor normalized channel models can be extended and used for other frequencies.**

I. INTRODUCTION

Wireless communications is one of the fastest growing fields in the communication engineering world. The increase in capacity of wireless communicating systems is still a constant goal in the mobile communication research area and many advanced radio techniques promising in terms of capacity have been deployed.

The evolutions of wireless systems based on a high spectral efficiency relate, among others, to two major topics: the improvement of the radio link by using MIMO configurations and the use of new frequency bands. For MIMO based systems, the system performance depends not only on the SNR, but also on the amount of spatial diversity the system can exploit [1, 2]. This spatial diversity relies on the delay and angular power profiles of the propagation channel and on their derived parameters like delay and angular spreads. As a result, a precise space-time propagation channel characterisation is required in order to evaluate the awaited profits of these techniques. 3D ray tracing based models can be used to predict the channel delay and angular profiles in a deterministic way [3], and hence provide the required spatio-temporal channel characterization.

This paper presents a comparison of the measured and predicted delay and angular spreads of UWB indoor channel parameters with some focus on their frequency dependence. Section II gives definitions of the delay spread and angular spread. Section III presents the channel simulation tool and an analysis of the relevant phenomena. Section IV describes the measurement set-up performed in a typical residential flat. The comparison between measured and predicted channel parameters and the influence of the frequency are presented in section V. We conclude this work with an overview of the results in section VI.

II. DEFINITION OF DELAY AND ANGULAR SPREADS

The delay spread σ_T characterizes the dispersion of the transmitted signal in time due to the time-dispersive influence of the channel. It is defined as the standard deviation of the delay values of the different paths, weighted proportional to the power in each corresponding path, i.e.,

$$\sigma_T = \sqrt{\frac{\sum_n (t_n - \bar{T})^2 . P_n}{\sum_n P_n}} \qquad (1)$$

$$\bar{T} = \frac{\sum_n t_n P_n}{\sum_n P_n}$$

where t_n and P_n are the delay and power of path n respectively.

The angular spread σ_θ characterizes the broadening of the transmitted signal in azimuth and elevation due to the angular-dispersive influence of the channel. The larger the angular spread, the higher is the space selecting fading. Note that the definition of angular spread is not as simple as that of delay spread, since angle is a periodic data. In this paper, we used the 3GPP definition of angular spread [4], which is the most commonly applied and it is calculated by:

$$\sigma_\theta = \min_\Delta \ \sigma_\theta(\Delta) \qquad (2)$$

$$\sigma_\theta(\Delta) = \sqrt{\frac{\sum_n (\theta_n + \Delta - \bar{\theta})^2 . P_n}{\sum_n P_n}}$$

$$\bar{\theta} = \frac{\sum_n (\theta_n + \Delta) P_n}{\sum_n P_n}$$

where P_n and θ_n are the power and angle of arrival or departure of path n respectively and Δ is a linear shift angle. We note that since the angular spread should be independent of a linear shift in the angles of arrival and departure, it should be the minimum of $\sigma_\theta(\Delta)$ over all Δ.

III. Modeling and Simulation

A. 3D Channel Simulation Tool

MATRIX is a 3D ray tracing software that calculates the ray paths between a given transmitter (Tx) and receiver (Rx). It is based on geometrical optics (GO) and the uniform geometrical theory of diffraction (UTD). The propagation phenomena taken into account are combinations of multiple transmissions, reflections and diffractions.

Since a detailed description of the 3D indoor environment is essential for a proper wave propagation modelling, we need to account for walls, floor, ceiling, windows and doors as well as some details such as furnitures. Plane facets with 3D dimensions describe indoor environment. Each facet is affected to a material which is characterized by its permittivity, conductivity and thickness. The electromagnetic properties of various building materials have been estimated in a previous study over the 2-16 GHz frequency band [5]. Consequently, MATRIX can operate over a large frequency range. In addition, it takes into account the UWB antenna including polarization and radiation pattern.

As a result, for a given Tx-Rx configuration, the simulation tool provides a list of all the identified ray paths. Each ray is characterized by its complex propagation vector, absolute delay, direction of arrival (DOA) and direction of departure (DOD). It is therefore possible to easily estimate spatio-temporal channel characteristics such as delay spread and angular spread.

Figure 1 shows an example of a 3D indoor scene with different ray paths found by MATRIX between the transmitter (Tx) and receiver (Rx).

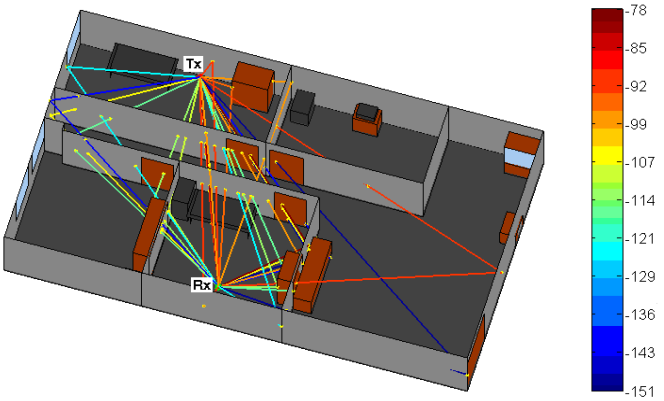

Fig. 1 An example of a 3D indoor scene with different ray paths found between the transmitter (Tx) and receiver (Rx)

B. Analysis of the Relevant Phenomena

It is known that ray tracing computation time increases rapidly with the number of reflection or diffraction phenomena. In order to reduce computation time, we have to compute useful paths only and ignore those without significant contribution to energy or any influence on the spatio-temporal channel parameters. For this purpose, we investigated on the evolution of both delay and angular spreads as a function of the number and type of phenomena taken into account. Also, different transmitter positions were considered in order to characterise the propagation channel in a residential environment.

Figure 2 represents the evolution of the delay spread and the azimuth and elevation angular spreads versus the type of added paths for 4 different transmitter positions. Each step on the horizontal scale corresponds to the addition of a new type

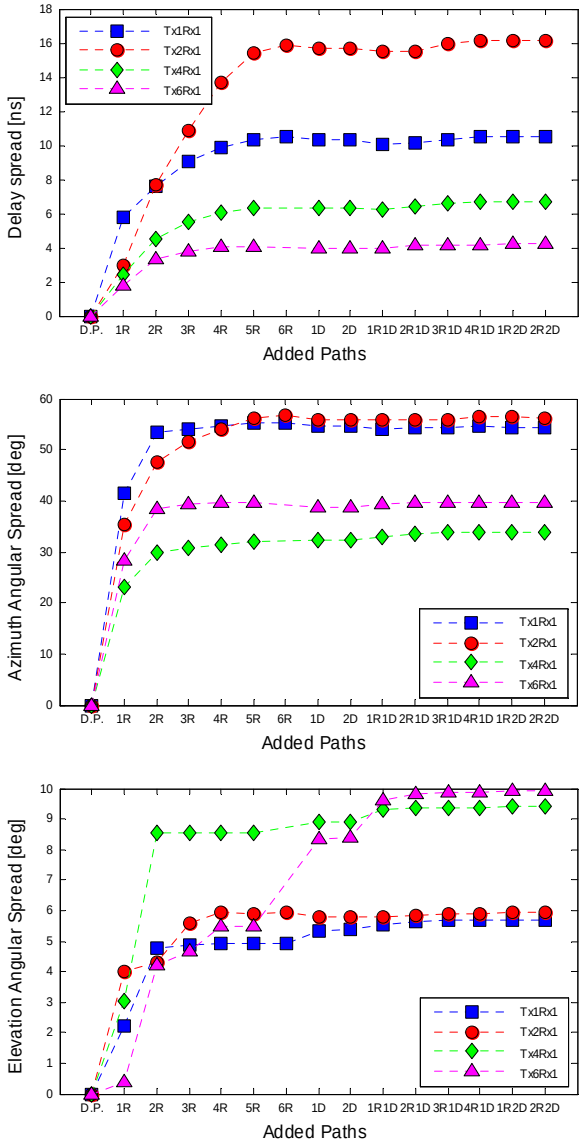

Fig. 2 Evolution of delay spread and azimuth and elevation angular spread vs. type of added paths: D.P. = Direct Path, R = Reflection, D = Diffraction

of path in the simulation. Paths containing reflexions were added first, then paths containing diffractions. Finally, paths containing a mix of reflexions and diffractions were considered. Note that a maximum of 6 transmissions have been allowed for every path. One can observe that graphs representing the evolution of the delay spread and azimuth angular spread of the two links Tx1Rx1 et Tx2Rx1 have the steepest slope. This is due to the fact that both links can be considered in NLOS situation when a concrete thick wall is present between transmitters and receiver. As direct paths are strongly attenuated, rays that do not impinge at that wall will have some significant contribution at the receiver in comparison to the direct path.

For most Tx positions, paths with six reflections or 2 diffractions or one diffraction and more than 3 reflections do not have any significant influence on the channel characteristics. For instance, they do not have any significant contribution to energy as their dynamic energy is 30 dB below the main path energy. Furthermore, the computation time required to find paths with a maximum of 6 reflections is 95 times larger than the time required to find paths with a maximum of 5 reflections. Also, it requires a computation time 160 times larger to find paths with one diffraction and maximum 4 reflections than to find paths with one diffraction and maximum 3 reflections. From the above observations, one can make some compromise between performance and computation time by only considering paths containing a maximum of 5 reflections or 2 diffractions, or one diffraction and maximum 3 reflections. Finally, a maximum number of 6 transmissions is allowed for each path. To evaluate the accuracy of our simulator, we compare hereafter the simulations to the measurements.

IV. Description of the Measurements

A. Measurement Set Up

The measurement equipment relies on two UWB circular arrays at both sides of the transmission link. A monocone UWB specific antenna, designed by Orange Labs, was used. Its construction is very simple and inexpensive. It is matched from 3 to 12 GHz with a VSWR (Voltage Standing Wave Ratio) value less then 2. A UWB array structure was introduced in [6], it combines a virtual uniform circular array (UCA) and a 5-axes monocone UWB antenna. It has been proved that the use of several antennas with particular orientations removes major drawbacks of classical uniform circular array. This setup offers some acceptable compromise between performance and complexity.

Propagation channel measurements were performed in frequency domain. The transmission channel was estimated with a VNA (Vector Network Analyser). Two LNA (Low Noise Amplifier) were used to improve the link budget. The MIMO configuration consists in measuring all links between all transmitting antennas toward all receiving antennas for each possible location. To reduce the experiment duration, only 3 antennas were measured at each side of the link. The radius of the UCA is 8 cm and the virtual location number was set to 60 to comply with Shannon sampling theory. The propagation channel was sampled over 4000 equally spaced frequencies between 2.5 and 12.5 GHz. It covers the FCC-defined frequency band for indoor UWB applications.

The whole measurement process was automated using specifically developed Matlab™ software. The schematic diagram of the measurements equipment is depicted in Fig. 3.

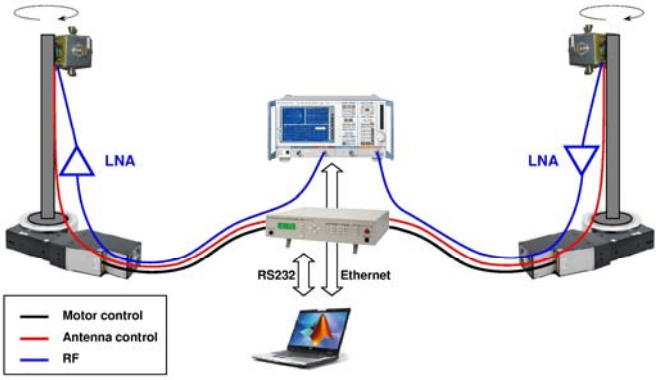

Fig. 3 Schematic diagram of the measurement equipment

B. Environment

An extensive UWB MIMO channel measurement campaign was carried out in a residential flat built inside the Orange labs premise [7]. This flat (see Fig. 4) is furnished and consists of 2 bedrooms, a kitchen, a desk room and a large living room. Thirteen different transmitter locations were investigated.

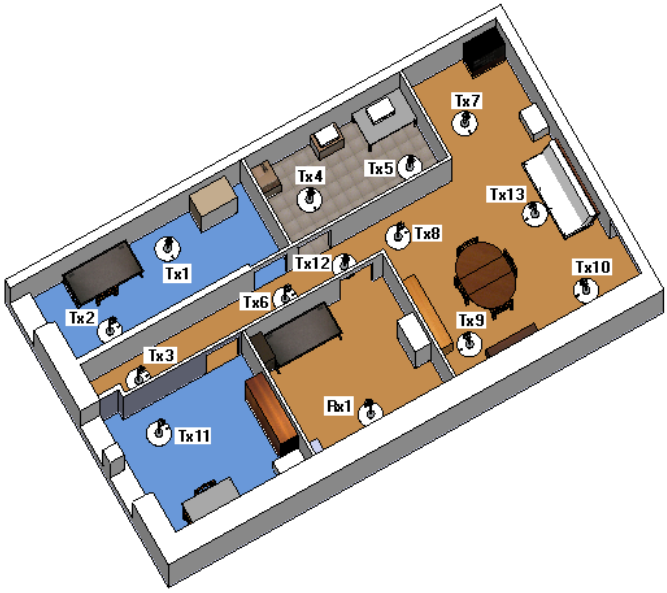

Fig. 4 A representation of the residential flat

V. Results

After subtracting the LNA transfer functions from the measurements, the calibrated transfer functions of the different MIMO configuration links are obtained. Different channel characteristics were then extracted, by considering

different central frequencies. To allow a fair comparison between measurements and simulations, we accounted for the influence of antennas and MIMO configuration in our simulations. For this purpose, we generated the channel transfer functions of the sets of rays simulated with MATRIX, according to the MIMO circular array configuration and antenna characteristics.

A. Power Delay Profile and Angular Delay Profile

The power delay profile (PDP) and the azimuth and elevation angular profiles (PAP) of the different MIMO configuration links were computed from the corresponding transfer functions. For each MIMO link, the power delay profile is considered as the average of the power delay profiles of all single input single output (SISO) links between the various transmitting and receiving antennas of the corresponding MIMO link. The azimuth and elevation power angular profiles at the receiver side of a MIMO link were considered as the average of the azimuth and elevation angular profiles of all single input multiple output (SIMO) links between the various transmitting and receiving antennas of the corresponding MIMO links. The power angular profile of the different single input multiple output links were computed by carrying out a directional analysis of the channel at all intervals of time to find the direction of arrival of rays within that interval. At each interval of time, a dynamic threshold of useful energy has been fixed in order to help reducing secondary lobe effects during beamforming.

Figure 5 represents the measured and simulated power delay profile and azimuth and elevation power angular profile of the link Tx6Rx1 for a central frequency equal to 6 GHz with 1- GHz bandwidth. Main paths have been found, but the simulated power delay profile and angular power profiles contain less energy than the measured ones. This may be due to our hypothesis that considers all reflections as specular reflections and ignores scattered signals. This underestimation of the power profiles will lead to underestimate in most cases the spatio-temporal channel characteristics as well, like delay and angular spreads.

B. Delay Spread and Angular Spread

The delay spread was computed from each collected power delay profile (PDP) whereas the azimuth and elevation angular spreads were computed from the corresponding power angular profiles (PAP). The delay spread and the angular spreads were computed over 8 sub-bands of 1 GHz each. The central frequencies of the selected bands extend from 3 to 10 GHz with one GHz step. Then, we computed both the average value and the standard deviation for the 8 sub-bands. As a result, it was possible to analyse the effect of the central frequency on the characteristics of the UWB propagation channel. Figure 6 illustrates the average measured and simulated delay spread, azimuth and elevation angular spreads at the receiver side of all Tx positions of the figure 4 against central frequency. For each band, the value of the standard deviation of each parameter is represented by the length of the vertical line.

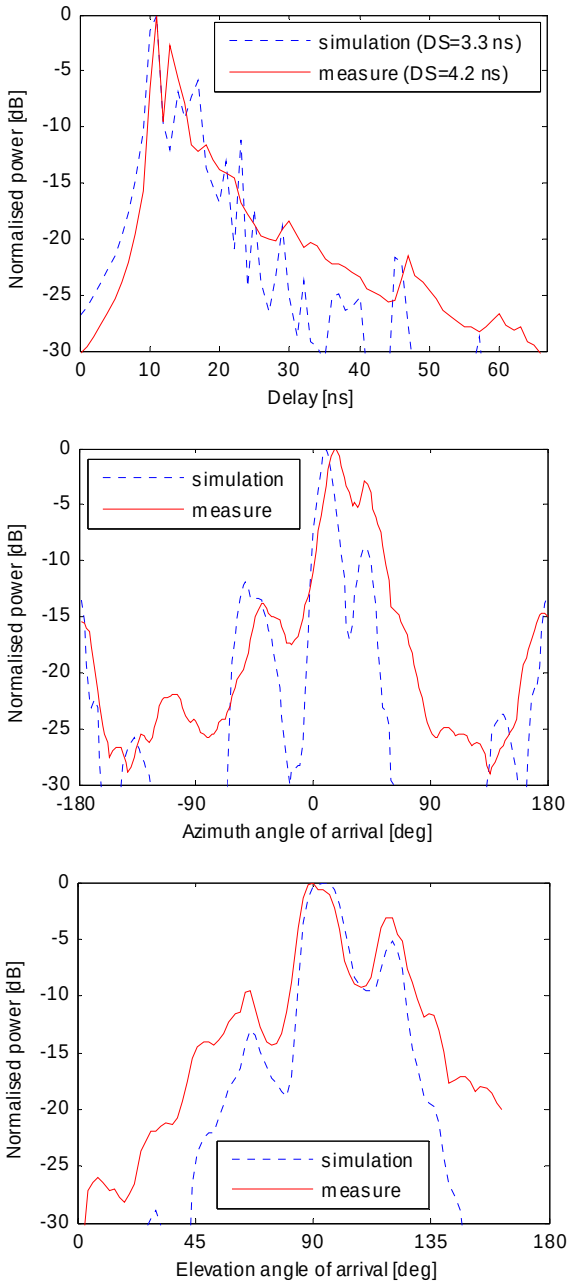

Fig. 5 Measured and simulated PDP and azimuth and elevation PAP of the link Tx6Rx1; the central frequency is 6 GHz with a bandwidth of 1 GHz

A small offset is observed between simulations and measurements. As expected, the predicted delay spread and azimuth and elevation angular spread values tend to be lower than the measured ones. Their values are in agreement with those reported by others [8, 9]. The occurrence of lower predicted delay spread values can be attributed partially to the absence of scattered signals from small furniture in our simulations as scattering may add significant energy more distributed in space into simulations. Besides, it is difficult to model exactly all the environmental details.

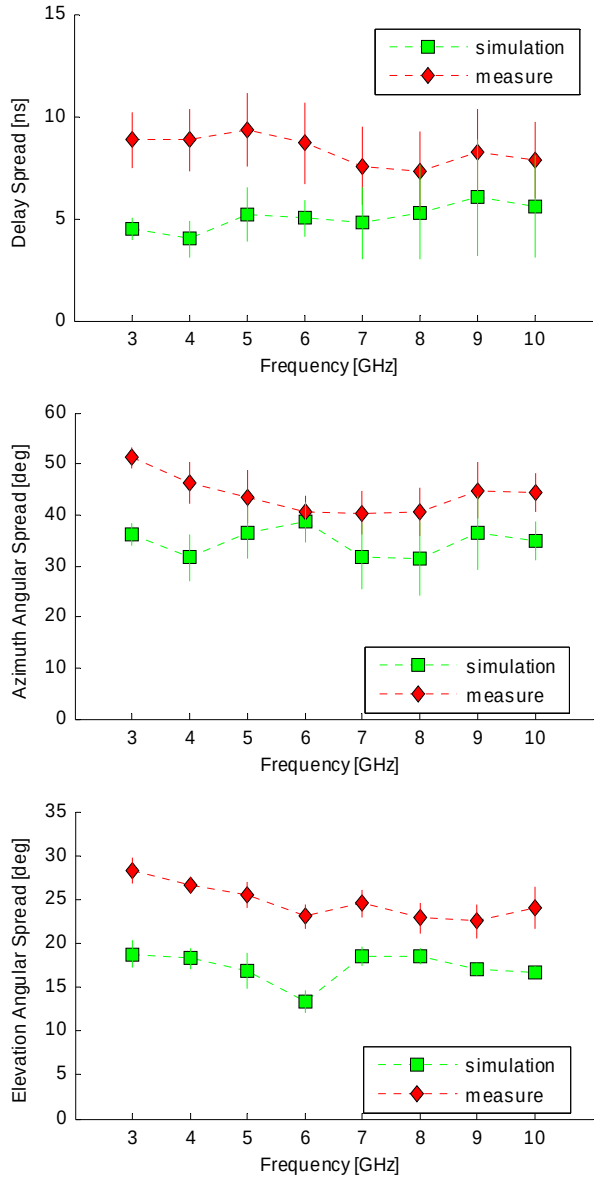

Fig. 6 Average measured and simulated RMS delay spread, azimuth and elevation angular spread and standard deviation of all Tx positions vs. central frequency

Concerning the frequency dependence of the parameters, we did not observe an obvious frequency dependence of the delay spread and the azimuth and elevation angular spreads. Their measured and predicted values are relatively stable over all frequencies from 3 to 10 GHz. A slight tendency to decrease with frequency is observed for the measured parameters. However, one can roughly consider their values as constant over all the frequency range. So an indoor channel model normalized for a frequency in the 3-10 GHz frequency band can be extended and used for other frequencies of this band.

VI. Conclusions

In this paper, we presented a comparison between measurements and 3D ray tracing predictions of MIMO UWB channel parameters in a residence. We showed also some specific interest on the frequency dependence of these parameters. The delay spread and the azimuth and elevation angular spread were computed over 8 sub-bands of 1 GHz each with central frequencies extending from 3 to 10 GHz.

A small offset is observed between measurements and simulations. Predicted values tend to be lower than measured ones. This may be due to the absence of scattered signals from small furniture in our simulations. The parameters did not present an obvious frequency dependence. Their values are relatively stable over all the frequency range. This implies that most of indoor normalized channel models can be extended for other frequencies in the 3-10 GHz frequency band.

Future works will focus on the comparison of MATRIX with other prediction tools and the addition of scattered waves to our simulations to have a better prediction of the UWB parameters.

References

[1] J. Winters, "On the Capacity of Radio Communication Systems with Diversity in a Rayleigh Fading Environment," *Selected Areas in Communications*, IEEE Journal on, vol. 5, pp. 871, 1987.

[2] G. J. Foschini and M. J. Gans, "On limits of wireless communications in a fading environment when using multiple antennas," *Wireless Personnal Communications*, vol. 6, pp. 311-335, 1998.

[3] O. Mantel, A. Bokiye, R. V. Dommele, and M. Kwakkernaat, "Measurement based verification of delay and angular spread ray-tracing predictions for use in urban mobile network planning," *COST Vienna*, Austria, September 2009/28-30.

[4] 3GPP-3GPP2 SCM AHG, "SCM-135: Spatial channel model text description", August 2003.

[5] G. Tesserault, N. Malhouroux, and P. Pajusco, "Multi-frequencies characterization of building materials: Angular and polarization analysis," presented at *European Conference on Antennas and Propagation*, 2007.

[6] P. Pajusco, G. Tesserault, N. Malhouroux, and C. Sabatier, "Novel array structure for space-time characterization of the UWB channel," presented at *Personal, Indoor and Mobile Radio Communications*, 2008. IEEE 19th International Symposium on, 2008.

[7] P. Pajusco, N. Malhouroux-Gaffet, and Y. Chartois, "Techniques de caractérisation ULB doublement directionnelle," presented at *JNM* 2009, Grenoble.

[8] F. TCHOFFO TALOM, "Modélisation déterministe du canal de propagation indoor dans un contexte Ultra Wide Band," vol. Ph.D. Rennes: INSA, 2005.

[9] T. Rautiainen, R. Hoppe, and G. Wolfle, "Measurements and 3D Ray Tracing Propagation Predictions of Channel Characteristics in Indoor Environments," presented at *Personal, Indoor and Mobile Radio Communications*, 2007. IEEE 18th International Symposium on, 2007.